BGSG

Volume 58

Research Paper

Correspondence to:
Georgios Chatzopoulos
ggh1983@hotmail.com

DOI number:
http://dx.doi.org/10.12681/bgsg.27155

Keywords:
Accelerating deformation, Thessaly, earthquake, Benioff strain

Citation:
Chatzopoulos, G. (2021), Accelerating Deformation Seismicity Patterns Before the March 3, 2021 Thessaly M_w 6.3 Strong Earthquake. First Results. Bulletin Geological Society of Greece, 58, 87-104.

Publication History:
Received: 01/06/2021
Accepted: 26/07/2021
Accepted article online: 29/07/2021

The Editor wishes to thank two anonymous reviewers for their work with the scientific reviewing of the manuscript and Ms Emmanouela Konstantakopoulou for editorial assistance.

ACCELERATING DEFORMATION SEISMICITY PATTERNS BEFORE THE MARCH 3, 2021 THESSALY M_W 6.3 STRONG EARTHQUAKE. FIRST RESULTS.

Georgios Chatzopoulos[1]

[1]Section of Geophysics – Geothermics, Department of Geology and Geoenvironment, National and Kapodistrian University of Athens, 15784 Panepistimiopolis, Athens, Greece,
ggh1983@hotmail.com.

Abstract

A widely felt strong shallow earthquake with Mw 6.3 magnitude occurred in Thessaly (Central Greece) on March 3, 2021. This recent strong event attracted our interest to apply and evaluate the capabilities of the Accelerating Deformation method. Based on the recently proposed generalized Benioff strain idea which could be justified by the terms of Non-Extensive Statistical Physics (NESP), the common critical exponent was calculated in order to define the critical stage before a strong event. The present analysis comprised a complex spatiotemporal iterative procedure to examine the possible seismicity patterns at a broad region and identify the best one associated with the preparation process before the strong event. The starting time of the accelerating period, the size and location of the critical area are unknown parameters to be determined. Furthermore, although, the time of failure is already known, in the present research it was not set as a fixed value in the algorithm to define the other unknown parameters but instead different catalogue ending dates have been tried out to be with an objective way. The broad region to be investigated was divided with a square mesh and the search of events around a point has been carried on with different size circular and elliptical shapes. Among the obtained results, the solution which exhibits the most dominant scaling law behavior as well as the one which exhibits the smallest spatial area and yet the more dominant scaling law behavior are presented.

***Keywords*:** *Accelerating deformation, Thessaly, earthquake, Benioff strain.*

Περίληψη

Ο πρόσφατος ισχυρός σεισμός μεγέθους ροπής Mw 6.3, την 3η Μαρτίου 2021, στην περιοχή της Θεσσαλίας αποτελεί μια ενδιαφέρουσα περίπτωση για την εφαρμογή της μεθόδου της επιταχυνόμενης παραμόρφωσης. Σύμφωνα με πρόσφατα ερευνητικά αποτελέσματα, η ερμηνεία της γενικευμένης παραμόρφωσης Benioff είναι δυνατό να τεκμηριωθεί με όρους Μη-Εκτατικής Στατιστικής Φυσικής και υποδεικνύει ένα κοινό κρίσιμο εκθέτη ο οποίος συμβάλει στον καθορισμό της κρίσιμης κατάστασης πριν από ένα ισχυρό σεισμό. Στην παρούσα εργασία εξετάστηκαν οι χωροχρονικές ιδιότητες της σεισμικότητας της ευρύτερης περιοχής με σκοπό να ανιχνευτούν πιθανά προσεισμικά πρότυπα, λαμβάνοντας ως παραμέτρους το χρόνο έναρξης της επιταχυνόμενης παραμόρφωσης καθώς και τη γεωμετρία και την έκταση της πιθανά κρίσιμης περιοχής. Για τον καθορισμό των σεισμών που πιθανά σχετίζονται με την υπό εξέταση σεισμική διέγερση, η περιοχή μελέτης χωρίστηκε σε τετραγωνικό πλέγμα και εξετάσθηκε η χρονική εξέλιξη της παραμόρφωσης Benioff σε κυκλικά και ελλειπτικά σχήματα στους κόμβους του πλέγματος. Παρά το ότι ο χρόνος γένεσης του σεισμού είναι γνωστός, η μελέτη πραγματοποιείται θεωρώντας τον ως μια υπό προσδιορισμό μεταβλητή. Από τα αποτελέσματα που προκύπτουν, παρουσιάζονται αυτά που έχουν την πιο σημαντική συμπεριφορά επιταχυνόμενης παραμόρφωσης καθώς και τα αποτελέσματα για μια μικρότερη σε διάμετρο κρίσιμη περιοχή τα οποία παρουσιάζουν εξίσου έντονη επιταχυνόμενη παραμόρφωση.

Λέξεις – Κλειδιά: *Επιταχυνόμενη παραμόρφωση, Θεσσαλία, σεισμός, παραμόρφωση Benioff.*

1. INTRODUCTION

A widely felt strong shallow earthquake with magnitude Mw 6.3 occurred in Thessaly (Central Greece) on March 3, 2021. This event rose scientific awareness due to the structural damages and the aftershock sequence with the several moderate and strong events during the first 48 hours. The Thessaly region exhibits faults capable for strong events up to M7.0 as that occurred in Sofades in 1954 (Papazachos and Papazachou, 2003). In this region and the surrounding areas, the dominant tectonic features are the normal faults with a NW-SE strike. According to the moment tensors of the mainshock and the two largest aftershocks occurred on 04/03/2021 and 12/03/2021 with M_w=6.0 and 5.6 respectively illustrated in Fig.1, the activated fault follows the same extensional stress regime of Thessaly region. This is also verified by the recent work of Ganas et al. (2021) where a detailed examination of the aftershock focal mechanism based on source

parameters from all the available reporting agencies is presented. The moment tensors in Fig.1 since 2003 with Mw equal or larger than 4.0 are from the revised database published by the National Observatory of Athens seismic network (NOA): doi.org/10.7914/SN/HL (accessed on 02/5/2021) as well as from the Global Centroid-Moment-Tensor (GCMT) (Ekström et al., 2012).

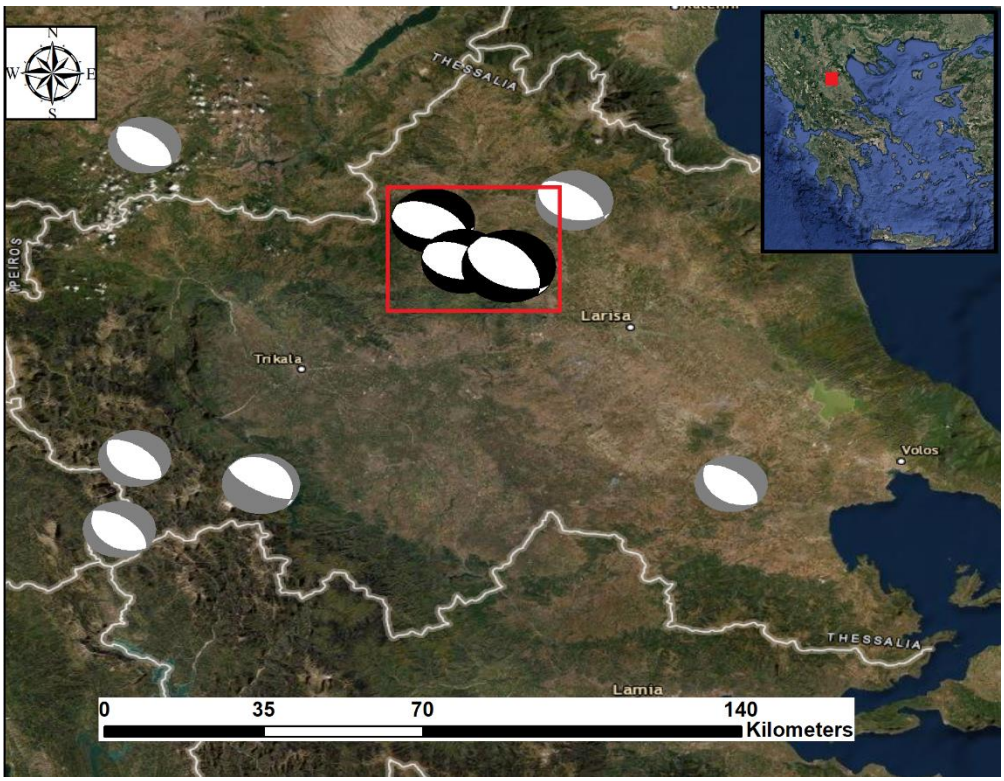

Fig.1: The moment tensors of the mainshock and the two strongest aftershocks (inside the red box) as well as of past events (noted with gray color in the surrounding region). Image from ArcGIS (www.arcgis.com, accessed on 11/07/2021), moment tensor illustration from Mirone software (Luis, 2007).

The recent large event in this area attracts our interest to apply and evaluate the applicability of the Accelerating Deformation method which is a widely used method based on the seismicity pattern observed before large events (Bufe and Varnes, 1993; Bowman et al., 1998; Papadopoulos et al 2000; Papazachos and Papazachos, 2000; Papazachos et al., 2005; Mignan and Di Giovambattista, 2008; De Santis et al., 2010 and references therein). Understanding the evolution of preseismic patterns related to the large earthquake parameters estimation and the seismic hazard mitigation is a scientific challenge. The hazard associated with large earthquakes, is attracting a vast number of researchers to study the preseismic indicators. Aiming to explain the observed seismicity patterns during the preparatory phase, theories that consider the large mainshocks as a critical point have been proposed. According to these ideas, in the deformed region, as the time progresses there is an increase in the number of events

usually with moderate magnitudes, which leads to a critical point, which is the completion of this preparation process (Sornette and Sornette, 1990; Jaume, S.C., Sykes, L.R., 1999; Rundle et al., 2000). Several studies have been focused on the fractal structure and properties of the faults and the fracture process have been correlated with hierarchical scaling laws (Lapenna et al., 2000; Di Giovambattista and Tyupkin, 2001; Scholz and Aviles 2013; Vallianatos and Chatzopoulos, 2018). An innovative approach to study the collective properties of earthquakes based on *Tsallis entropy* (Tsallis, 2009; Vallianatos et al., 2016) who used a generalized concept of the Boltzmann-Gibbs statistical mechanics. Tsallis used this concept to study the seismicity as dynamical systems that exhibit memory effects, long range correlations and multifractality. Based on the Tsallis non-extensive statical physics, a theoretical model to address the scaling laws as that of Benioff strain evolution for large earthquake preparation mechanisms was proposed (Vallianatos and Chatzopoulos, 2018 and references therein). In the present work, an effort to investigate the possible seismicity patterns before the Thessaly first strong event (M_w=6.3) with the ideas of Accelerating Deformation as recently formulated in Vallianatos and Chatzopoulos (2018) is presented.

2. METHODS AND DATA

In the Accelerating Crustal Deformation method, the energy release during the preparation phase of a large earthquake expressed by an accelerating – decelerating seismic crustal deformation scalar equation (Bufe and Varnes, 1993):

$$\Omega(t) = \Omega_f - B(t_f - t)^m, \qquad \textbf{(1)}$$

where t is the preparation time before the origin time (t_f) of the termination event i.e., the mainshock, Ω_f is the cumulative strain energy at t_f while B, and m are model parameters. The critical exponent m takes values close to 0.3 for accelerating energy according to several theoretical and laboratory results (Brehm and Braile 1999; Ben-Zion and Lyakhovsky, 2002), close to 1 for background seismicity while values larger than 1 characterize deceleration seismicity patterns.

A considerable number of researchers (Bufe and Varnes, 1993; Bowman, et al., 1998; Brehm and Braile, 1999; Papazachos and Papazachos, 2000; Rundle, et al., 2000; Scordilis et al., 2004; Di Giovambattista and Tyupkin, 2004; Mignan and Di Giovambattista, 2008; De Santis et al., 2010; Papadopoulos and Minadakis, 2016 and references therein) studied the preshock seismicity patterns with the most common

measuring quantity the cumulative square root of seismic energy known as Benioff strain. The cumulative Benioff strain, $\Omega(t)$ for n events at the time t:

$$\Omega(t) = \sum_{i=1}^{n(t)} E_i^{1/2}(t), \quad \textbf{(2)}$$

where E_i is the seismic energy of the to ith event. The energy can be estimated from the magnitude. The validated empirical relation energy (E) versus moment magnitude (M) for the Greek region proposed by Papazachos and Papazachos (2000), was applied:

$$\log E = 1.5 * M + 4.7. \quad \textbf{(3)}$$

To define the beginning of the acceleration period, (the time when the power law scaling starts and express the deviation from linearity which characterizes the background seismicity pattern) the Curvature parameter (Cp) have been proposed by Bowman et al. (1998):

$$Cp = (Power\ law\ fit\ RMS)/(Linear\ fit\ RMS). \quad \textbf{(4)}$$

As the Cp becomes smaller approaching to zero, the scaling law behavior becomes dominant and a typical value less than 0.70 have been suggested by Bowman et al. (1998) as a robust indication of accelerating seismicity.

In the recent work of Vallianatos and Chatzopoulos (2018), analytical expressions with terms of Non-Extensive Statistical Physics (NESP) have been formulated to propound a theoretical framework that describes the physical processes of the energy flow and accumulation inside a crustal volume. The NESP ideas considered as a suitable approach as they can explain the long-range temporal dependence of seismicity in a fault system that obeys a hierarchical distribution (Scholz and Aviles, 2013; Michas et al., 2015). Vallianatos and Chatzopoulos (2018) introduced the generalized cumulative Benioff deformation,

$$\Omega_\xi(t) = \sum_{i=1}^{n(t)} E_i^{\xi}(t), \quad \textbf{(5)}$$

where $0 \leq \xi \leq 1$. When the energy exponent ξ is equal to 0, then the quantity $\Omega_0(t)$ is the cumulative number of earthquakes till the time t. For ξ equal to 0.5, the $\Omega_{0.5}(t)$ is the well-known cumulative Benioff strain while for ξ equal to 1, the quantity $\Omega_1(t)$

represents the cumulative energy released. They applied a non-extensive statistical physics approach and concluded to the equivalent power law equation:

$$\Omega_\xi(t) = \Omega_{\xi f} - B(t_f - t)^{m_\xi}, \quad \textbf{(6)}$$

where t is the time before the time of failure t_f and when $t = t_f$ the Ω_ξ is equal to $\Omega_\xi(t_f)$, B is a model parameter and m_ξ is the critical exponent. This approach suggests that during the accelerating seismic pattern for $0 \leq \xi \leq 1$ there is a common critical exponent $m_\xi \approx 0.30$ which is independent of the ξ-value of the generalized Benioff strain $\Omega_\xi(t)$.

According to Vallianatos and Chatzopoulos (2018), the entropy parameter q determines the cumulative fractal distribution of seismic subvolumes of preshocks inside a stressed crustal volume V, with fractal dimension $d = d_e \frac{2-q}{q-1}$, where d_e the Euclidean dimension. Following the equation 10c of Vallianatos and Chatzopoulos, (2018):

$$m_\xi = \alpha(d_e - 1 - d) + 1 \quad \textbf{(7)}$$

the m_ξ depends on the Euclidean dimension d_e of the stressed crustal volume V of the earthquake preparation region and the NESP entropy parameter q. By considering a 3D spatial distribution $(d_e = 3)$ of EQs during the preparation phase $(t < t_f)$ the entropy parameter is constrained to take values between $\frac{7}{4}$ and 2 whereas for the 2D case (e.g., a very shallow seismogenic layer) the entropy parameter is constrained to values $\frac{5}{3} < q < 2$ (Vallianatos and Chatzopoulos, 2018). In any case, the earthquake source region is a complex, sub-additivity seismic system characterized by long-range temporal correlations among earthquakes.

Based on the remark that there is common critical exponent m_ξ, which is independent of the ξ, the M_w=6.3 (March 3, 2021) mainshock occurred in Thessaly has been examined for the existence of accelerating seismicity patterns. Although, this analysis has been carried out in a retrospective manner and the time of failure (t_f) is already known, the latter did not take a fixed value, and it has been estimated from the algorithm along with the other power law relation parameters. The aim was to examine all the possible variables such as the starting time of the accelerating seismicity pattern as well as the size and the location of the critical area in order to evaluate them along with the estimated t_f.

Since no recent large earthquakes occurred in the broad region under investigation, to pursuit the starting time and define the acceleration period, it was necessary to use an earthquake catalogue with long time history. Based on the previous published work for the Accelerating Deformation method (Papazachos and Papazachos, 2000; Di Giovambattista and Tyupkin, 2004; Papazachos et al., 2005), a few years to a couple of decades is reported as a typical duration of the preparatory phase for an event of such a magnitude. To this end, as time, t elapses since 2005, a cumulative procedure with a monthly iteration step was implemented to study the recent strong event in Thessaly. The generalized Benioff strain analyses were conducted on the earthquake catalogue provided by the Permanent Regional Seismological Network operated by the Aristotle University of Thessaloniki, registered in the International Federation of Digital Seismograph Networks with doi:10.7914/SN/HT (accessed on 02/05/2021). This is an open access manually revised catalogue, and it has been adopted for this research. The earthquake catalogue is the input data for the Accelerating Deformation method. Its quality relies on the data completeness and its accuracy on the of the earthquake parameters (epicenter, origin time, depth).

The data completeness of the catalogue has been carried out by examining the Magnitude of completeness, M_c which is based on Gutenberg-Richer law and defines the lowest magnitude value of a dataset in which all earthquakes were detected (Mignan and Woessner, 2012). The spatial variation of M_c for the examined period (since 2005) and region (descripted in the next paragraph) is much less than 3.0, calculated using geographical coordinates with grid size 0.1 degrees with 50 events and 50 bootstraps method with the “best combination” option in ZMAP software (Wiemer, 2001) which uses the Max Curvature, Goodness of Fit 90 and 95% confidence techniques (Wyss et al., 2001). The temporal variations of M_c for the research area present a peak close to 3.1 in the end of 2008. Considering the M_c examination results, a range cut-off for the earthquake magnitudes, Mcut with values from 4.9 down to 3.2 was applied to investigate the possible seismicity patterns based on the Mcut changes. Furthermore, due to inherent significant uncertainty of earthquakes depths, posing a depth parameter limit to refine the earthquake catalogue may have negative impact to the identification of the accelerated crustal volume. Thus, different depth cut-off values (Dcut) were tested, starting from 25 km down to 40 km, with an iteration mode, initially with a 5 km step and afterwards with a 2.5 km.

Towards identifying the location of the deformed crustal volume that presents critical point characteristics, the broader region around the epicenter of the mainshock (from

N38.50° to N41.0° and from E21.00° to E23.50°) was initially divided in a square mesh with 0.05 degrees size as a first approximation search to point out the locations with a possible result. Subsequently the search was repeated with a denser square mesh (0.02 degrees size) around these locations with a preliminary seismic pattern identification. In this way, the processing time as well as the computing power needed for algorithm to carry out the whole iterative procedure, were dramatically reduced. At every mesh point, an iterative expanding circular area was shaped with the use of the Euclidean distance to find the surrounding events. The circle varies in diameter from 40 to 300 km with an initial step 4 km which was reduced to 2 km for a more comprehensive second scan. Earth's shape was considered in the calculations of distances. In an attempt to reveal directional (strike) properties of the critical area, resulted from the above circular (symmetrical) approximation, the iterative algorithm continues using elliptical shapes. Around the center of the identified circular critical area, an ellipse is tried out, using the same parameters such as time window, magnitude and depth cut-offs values. The size of the ellipses axes has been set to take values from 40 km up to 300 km with a 4 km step and the primary axis is rotated in the horizontal plane from 0 to 180 degrees with a 15 degrees step.

Regarding the application of Curvature parameter criterion, the seismic pattern solutions were initially screened with $C_p \leq 0.55$, which is a rational value based on the experience built-up by examining other case studies, and on-going analysis to narrow down the results led to $C_p \leq 0.50$, as lower Cp-values indicate higher degree of deviation from the background seismicity. To achieve a valid regression analysis, both for power law and linear fittings, the minimum number of events in a possible seismic pattern solution was set to 30. During the mesh scan, when the latter statistical threshold was satisfied for the events around a point, then the algorithm performed three individual sets of power law and linear fitting, one for each ξ generalized Benioff strain function exponent 0, 0.5 and 1. Preliminary identifications were considered those who exhibited critical exponents, m_ξ with values 0.30±0.05 for the same time-window, circle size and number of events. Among these solutions, to retrieve those with the more accurate regression analysis, and since the algorithm delivers three sets of power law - linear fittings and three Cp-values, the results that did not demonstrate the smallest Curvature parameter mean value were filtered out. Furthermore, adopting the reasonable seismological hypothesis that the seismicity associated with the critical phenomenon is expected to be spatially concentrated, between the results with the same Cp mean-value, the ones delivering the smallest critical areas have been selected. Lastly, to examine the quality and robustness of the power law fitting, the square of the Pearson correlation coefficient (r) was used between each cumulative quantity ($\Omega_\xi(t)$)

and the corresponding power law fitting and accepted results were considered the ones that presented $r \geq 0.977$.

3. RESULTS

The first approach to identify the stressed critical volume with circular areas around a mesh point demonstrated values for Mcut from 3.2 up to 3.6. The analysis showed that all the circle centers with a possible solution form two clusters and are located north of the mainshock's epicenter while the majority of the associated events are North-Westerly from the epicenter. The possible solutions produced, present circles with diameter ranging from 190 to 280 km. The best two (with the lowest mean Cp value) circular seismic pattern solutions for the largest Mcut available (Mcut=3.6) are comparatively presented and discussed here.

The first one, (named hereafter as CAA) focuses on the overall smallest Cp mean-value while the other one (named hereafter as CAB) is aftermath of constraining circle diameter up to 200 km. The circular critical area A achieved $m_\xi = 0.30 \pm 0.05$ with the lowest Cp mean-value along with its generalized Benioff strain power law and linear fitting with ξ-values 1, 0.5 and 0 are presented in Fig. 2. The circle center has geographical coordinates N40.40°, E22.00° and the circle diameter is 252 km, the latter to be perceived as an indicative numerical result and not an exact value of a seismotectonic feature or behavior. The determined time window of accelerating seismicity (the main earthquake preparation period) for this solution includes events since the second half of 2009. The circular critical area CAB resulted by posing upper limit to its size, again along with its generalized Benioff strain power law and linear fitting for ξ values 1, 0.5 and 0 respectively and critical exponent $m_\xi = 0.30 \pm 0.05$ are illustrated in Fig. 3. The circle center has now geographical coordinates N40.74°, E21.64°, moved ~48 km away and heading NW 320° from that of CAA solution, the circle diameter is 192 km and the time window includes events since the second quarter of 2008. For the shake of completeness, the seismicity in the investigated broad region around the main event which has not been correlated with the critical area since 2008, is also presented in both figures (illustrated with black circles). It comprises events with local magnitude equal to or greater than Mcut =3.6 up to 5.0. Based on the n extensive experimentation and trials on other studied cases, the generalized Benioff strain with ξ=1 (the release of cumulative of seismic energy) usually achieves a better estimation for the occurrence time of failure (t_f). This consistency concept appears also in this research, where for the solution CAA the cumulative energy release has the more accurate estimation of failure time (08-Mar-2021) (Fig. 2b) just a few days after the

actual occurrence time of the strong earthquake while for CAB solution provides an estimation of t_f a few weeks ahead (23-Mar-2021) (Fig. 3b).

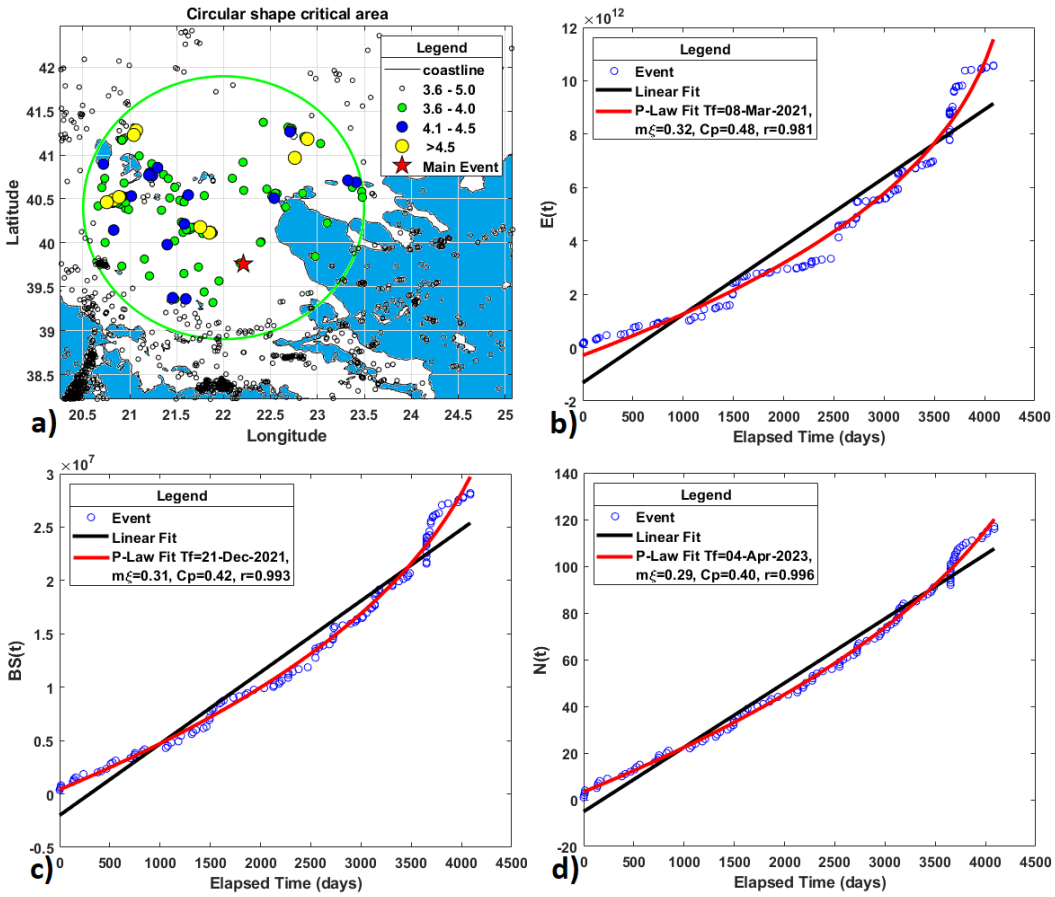

Fig. 2: a) Map with the circular critical area approach based on mean Cp criterion as well as the rest seismicity (see text for details). The first strong earthquake is denoted with a red star while the magnitudes of the events associated with the critical area are represented with circles with different color and size. The generalized Benioff strain (red curve) and the linear fitting (black line) for: b) the cumulative energy released (ξ=1); c) the cumulative Benioff strain (ξ=0.5); d) cumulative number of earthquakes (ξ=0).

The robustness of the solution CAA is justified by the results acquired by selecting Mcut equal to 3.5, thus more earthquakes are included. A similar seismic pattern solution was produced with the same geographical coordinates and size of circular critical area but the estimation of failure time (19-02-2021) is almost two weeks before of that of the CAA solution. By selecting Mcut equal to 3.4, the solution is compatible to CAA, the circle center has geographical coordinates N40.54, E21.74, circle diameter 198 km while the estimation of failure time is just a week before of that of CAA. The application of the depth cut off filter on the studied earthquake catalogue proved to have

no influence on the CAA and CAB solutions as all the events associated with their determined critical areas are featured by shallower hypocenters.

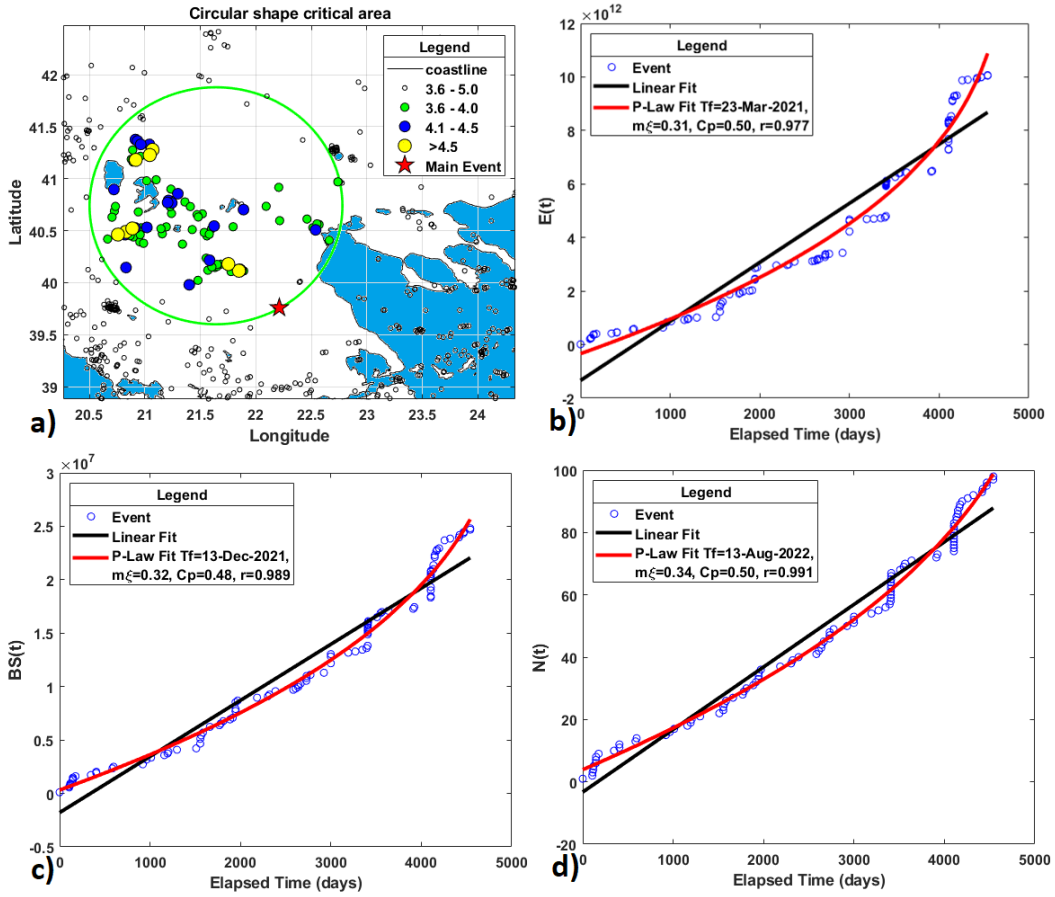

Fig. 3: a) Map with the circular critical area approach with the small radius as well as the rest seismicity (see text for details). The first strong earthquake is denoted with a red star while the magnitudes of the events associated with the critical area are represented with circles with different color and size. The generalized Benioff strain (red curve) and the linear fitting (black line) for: b) the cumulative energy released (ξ=1); c) the cumulative Benioff strain (ξ=0.5); d) cumulative number of earthquakes (ξ=0).

An additional alternative effort to evaluate the validity of the obtained results and yet more to reveal the long-range correlations in seismicity of a critical crustal volume under accelerating deformation was exercised by searching the area for seismicity patterns with different, earlier than the main event, ending dates. The earthquake catalogue was shrunk from its bottom (events backward in time were progressively removed) as the ending date of the catalogue was successively sent to the past with an iterative 10-day step. This method pushes artificially the seismic pattern identification

iterative procedure in a previous date. At every iteration, a monthly iteration step since 2005 was implemented to point out the starting point for the accelerating deformation period but this time with a "new" ending point moved further in the past of the main event's actual occurrence time. This iterative catalogue reduction test showed that the obtained results were the same since 10-Aug-2020 signifying that after that date there were no new events with magnitude equal or larger than Mcut in the identified critical area.

Taking the aforesaid iteratively optimized results for the circular critical area approximation into account, the same algorithmic procedure with an elliptical (asymmetric) approximation was applied. This approach aims to investigate probable striking properties of the critical seismic area subjected by a non-uniform stress regime, as in the case of Thessaly basin being under a regional extensional stress with N-S direction (Caputo, and Pavlides, 1993). To this end, the critical area search with the elliptical shape approximation, was executed in a region limited around the previous solutions using the same time-window and criteria (m_ξ = 0.30±0.05, Cp ≤0.50, D_{cut}, M_{min} = 3.6, and r ≥0.977). Again, the results obtained by applying the smallest Curvature Parameter mean-value criterion. The elliptical critical area identified, adopting the CAA solution parameters, along with the generalized Benioff strain power law and linear fittings with ξ-values 1, 0.5 and 0 respectively, are depicted in Fig. 4. The elliptical area center has geographical coordinates N40.44° and E22.08° (compatible with those of CAA), the principal axes have lengths 268 km and 244 km respectively, and the ellipse azimuth is 0 degrees. The estimated time of failure (01-04-2021) based on the cumulative energy release (ξ=1) (Fig. 4b) is almost a month later than the actual, so much less successful than of CAA. The results from this analysis do not significantly improve the image of the critical area and they do not point out any prominent striking as the output ellipse is practically a circle (flattening value 0.09).

The elliptical critical area identified, adopting the CAB solution parameters, along with the generalized Benioff strain power law and linear fittings with ξ-values 1, 0.5 and 0 respectively, are depicted in Fig. 5. The elliptical area center has geographical coordinates N40.40°, E21.64° (moved ~33 km to the south from that of CAB south and surprisingly matching the geographical latitude of the center of both the circle and ellipsis from CAA), the principal axes have lengths 256 km and 164 km, respectively, and the ellipsis azimuth is 165 degrees. The estimated time of failure (02-03-2021) is the most accurate one among the all the results, always coming out from the generalized Benioff strain with ξ=1 (Fig. 5b).

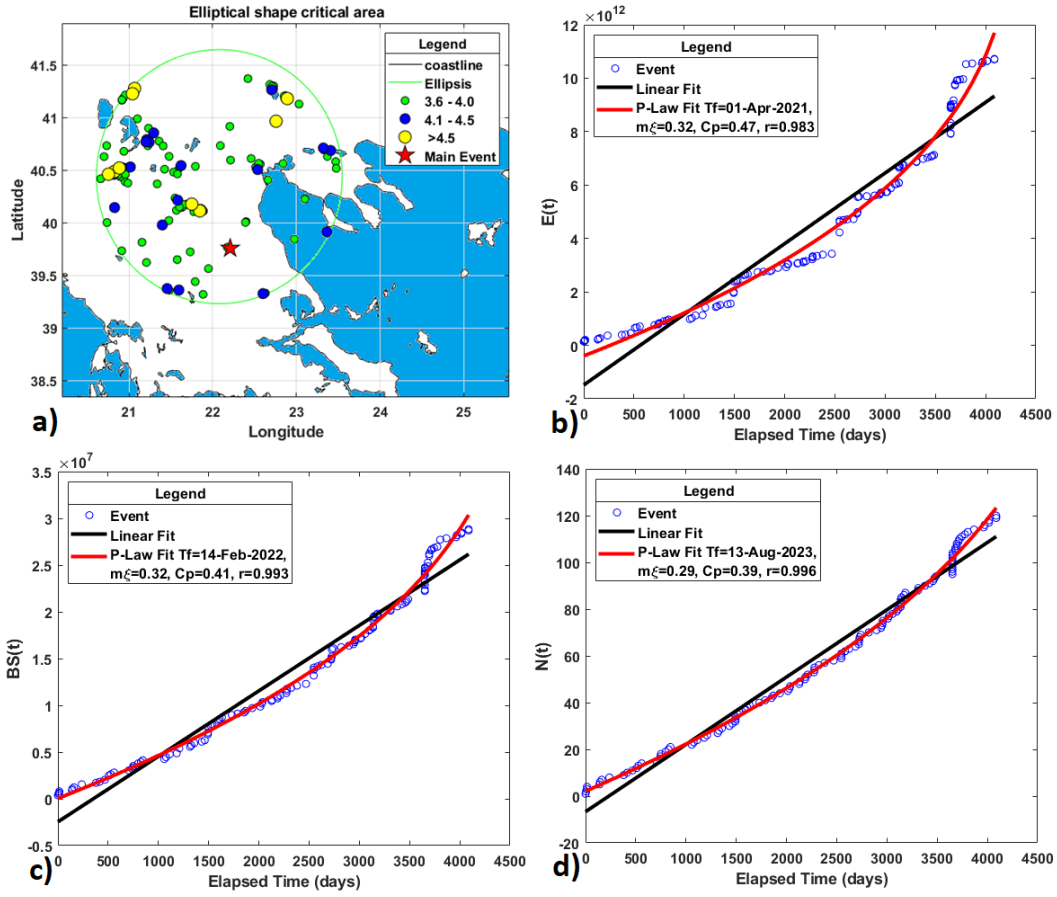

Fig. 4: a) Map with the elliptical critical area approach based on 'CAA' solution. The first strong earthquake is denoted with a red star while the magnitudes of the events associated with the critical area are represented with circles with different color and size. The generalized Benioff strain (red curve) and the linear fitting (black line) for: b) the cumulative energy released (ξ=1); c) the cumulative Benioff strain (ξ=0.5); d) cumulative number of earthquakes (ξ=0).

4. CONCLUDING REMARKS

Following a complex spatiotemporal iterative procedure to examine the possible seismicity patterns, it is shown that the recently proposed ideas for the generalized Benioff strain can explain and identify accelerating seismicity patterns before the M_w=6.3 strong Thessaly earthquake. The generalized Benioff strain with the common critical exponent criterion $m_\xi = 0.30 \pm 0.05$ can provide results for different earthquake magnitude cut-off values. The Mcut investigation for the possible seismicity patterns shown that small changes in the Mcut value will present results with similar identified critical area spatial properties but the larger Mcut values appear to have more accurate results in terms of time of failure estimation. Thus, setting the Mcut value to allow smaller magnitudes then it is necessary to enhance the searching resolution details and in this case the quality of the catalogue has to be considered.

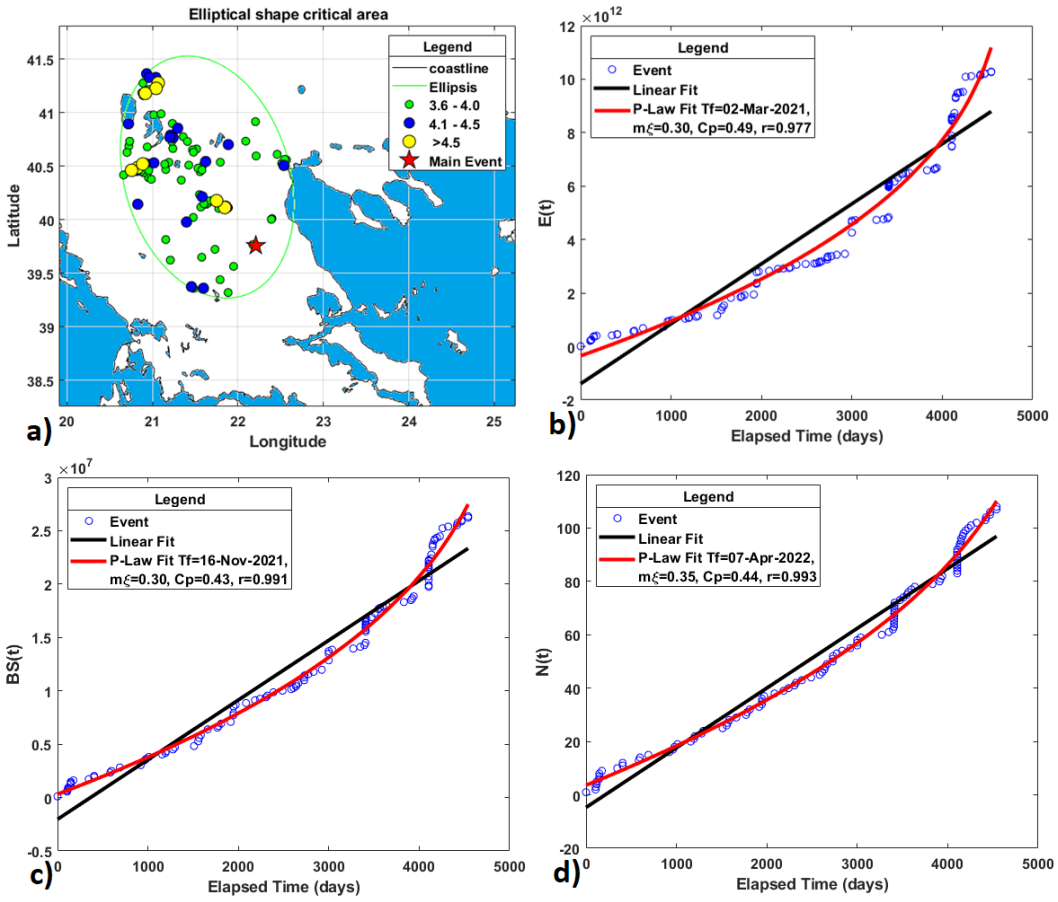

Fig. 5: a) Map with the elliptical critical area approach based on 'CAB' solution. The first strong earthquake is denoted with a red star while the magnitudes of the events associated with the critical area are represented with circles with different color and size. The generalized Benioff strain (red curve) and the linear fitting (black line) for: b) the cumulative energy released (ξ=1); c) the cumulative Benioff strain (ξ=0.5); d) cumulative number of earthquakes (ξ=0).

A number of criteria have been applied to improve the solutions robustness. The mean-value Curvature parameter criterion Cp ≤0.50 defines a critical area dominant scaling law behavior while the square of the Pearson correlation coefficient ($r \geq 0.977$) helps to have accurate fittings. The successive stage procedure to search first for circular and then for elliptical shape critical areas aims to reduce the processing time and increase the computing power efficiency.

The time of failure estimation obtained from the power law fitting for the present Accelerating Deformation study case, is better for ξ=1 (cumulative seismic energy) as it is closer to the actual occurrence time of the mainshock. The rest ξ exponents (ξ=0.5 and 0) provide a not so accurate time of failure estimation. Based on the experience built-up by examining other case studies, the rest ξ exponents usually estimate the time

of failure in the more distant future, but for this case the difference between estimations is significant. This is a matter that will be addressed again in a future work with more examples.

Both approaches (symmetrical and non-symmetrical), applied successively, produce compatible results. The CAA and CBB best solutions for circular (symmetrical) critical areas provide results with similar spatiotemporal properties. As the elliptical (non-symmetrical) approximation is subsequently applied on the outputs of the best circular areas, the constrained circle size of CBB favors the asymmetric approach results. The results for the asymmetrical (elliptical) approximation for CAA solution point out as the best option an ellipsis with small flattening (0.09) which has an estimation for failure time almost a month later than the actual origin time. On the contrary, the elliptical approach for CAB solution appears to provide the most promising result. The majority of the events associated with the critical area and the mainshock are concentrated in a narrow area with NW-SE strike and North-Westerly of the mainshock's epicenter. The ellipse for CAB solution follows the Thessaly basin regional extensional stress regime and has the most accurate estimated time of failure.

5. ACKNOWLEDGMENTS

This research is co-financed by Greece and the European Union (European Social Fund-ESF) through the Operational Programme «Human Resources Development, Education and Lifelong Learning» in the context of the project "Reinforcement of Postdoctoral Researchers - 2nd Cycle" (MIS-5033021), implemented by the State Scholarships Foundation (IKY).

6. REFERENCES

Ben-Zion, Y. and Lyakhovsky, V., 2002. Accelerated Seismic Release and Related Aspects of Seismicity Patterns on Earthquake Faults. *Pure and Applied Geophysics*, 159, 2385–2412 https://doi.org/10.1007/s00024-002-8740-9

Bowman, D. D., Quillon, G., Sammis, C.G., Sornette, A. and Sornette, D., 1998. An observational test of the critical earthquake concept. *Journal of Geophysical Research*, 103, 24359 – 24372 doi:10.1029/98JB00792.

Brehm, D.J., and Braile, L.W., 1999. Refinement of the modified time-to-failure method for intermediate-term earthquake prediction. *Journal of Seismology*, 3, 121 – 138. https://doi.org/10.1023/A:1009859431834

Bufe, C.G. and Varnes, J.D., 1993. Predictive Modeling of the Seismic Cycle of the Greater San Francisco Bay Region. *Journal of Geophysical Research*, 10, 9871–9883.

Caputo, R. and Pavlides, S., 1993. Late Cainozoic geodynamic evolution of Thessaly and surroundings (central-northern Greece). *Tectonophysics*, 223, 3–4, 339-362.

Di Giovambattista, R. and Tyupkin, Y., 2001. An analysis of the process of acceleration of seismic energy emission in laboratory experiments on destruction of rocks and before strong earthquakes on Kamchatka and in Italy. *Tectonophysics*, 338, 339–351.

Di Giovambattista, R. and Tyupkin, Y., 2004. Seismicity patterns before the M=5.8 2002, Palermo (Italy) earthquake: seismic quiescence and accelerating seismicity. *Tectonophysics*, 384, 243 - 255.

De Santis, A., Cianchini, G., Qamili, E. and Frepoli, A., 2010. The 2009 L'Aquila (Central Italy) seismic sequence as a chaotic process. *Tectonophysics*, 496, 44–52.

Ekström, G., Nettles, M. and Dziewonski, A.M., 2012. The global CMT project 2004-2010: Centroid-moment tensors for 13,017 earthquakes. *Physics of the Earth and Planetary Interiors*, 200-201, 1-9, doi: 10.1016/j.pepi.2012.04.00

Ganas, A., Valkaniotis, S., Briole, P., Serpetsidaki, A., Kapetanidis, V., Karasante, I., Kassaras, I., Papathanassiou, G., Karamitros, I., Tsironi, V., Elias, P., Sarhosis, V., Karakonstantis, A., Konstantakopoulou, E., Papadimitriou, P., & Sokos, E.,2021. Domino-style earthquakes along blind normal faults in Northern Thessaly (Greece): kinematic evidence from field observations, seismology, SAR interferometry and GNSS. *Bulletin Geological Society of Greece*, 58, 37-86. https://doi.org/10.12681/bgsg.27102

Jaumé S.C., Sykes L.R. 1999. Evolving Towards a Critical Point: A Review of Accelerating Seismic Moment/Energy Release Prior to Large and Great Earthquakes. In: Wyss M., Shimazaki K., Ito A. (eds) Seismicity Patterns, their Statistical Significance and Physical Meaning. Pageoph Topical Volumes. Birkhäuser, Basel. https://doi.org/10.1007/978-3-0348-8677-2_5

Lapenna V., Macchiato M., Piscitelli S., Telesca L. 2000. Scale-invariance Properties in Seismicity of Southern Apennine Chain (Italy). In: Blenkinsop T.G., Kruhl J.H., Kupková M. (eds) Fractals and Dynamic Systems in Geoscience. Pageoph Topical Volumes. Birkhäuser, Basel. https://doi.org/10.1007/978-3-0348-8430-3_7

Luis, J., 2007. Mirone: A multi-purpose tool for exploring grid data. Computers & Geosciences, 33, 31-41.

Michas, G., Vallianatos, F., Sammonds, P., 2015. Statistical Mechanics and scaling of fault population with increasing strain in the Corinth Rift. *Earth Planetary Science Letters*, 431, 150–163 https://doi.org/10.1016/j.epsl.2015.09.014 .

Mignan, A. and Di Giovambattista, R., 2008. Relationship between accelerating seismicity and quiescence, two precursors to large earthquakes. *Geophysical Research Letters*, 35, L15306 doi:10.1029/2008GL035024.

Mignan, A. and Woessner, J., 2012. Estimating the magnitude of completeness for earthquake catalogs. *Community Online Resource for Statistical Seismicity Analysis*, Version: 1.0, pp. 1 – 45.

Papadopoulos, G.A., Drakatos, G. & Plessa, A., 2000. Foreshock activity as a precursor of strong earthquakes in Corinthos Gulf, Central Greece. *Physics and Chemistry of the Earth, Part A: Solid Earth and Geodesy*, 25(3), 239 - 245.

Papadopoulos, G.A. and Minadakis, G., 2016. Foreshock Patterns Preceding Great Earthquakes in the Subduction Zone of Chile. *Pure and Applied Geophysics*, 173, 3247–3271. https://doi.org/10.1007/s00024-016-1337-5

Papazachos, B. and Papazachos, C., 2000. Accelerated Preshock Deformation of Broad Regions in the Aegean. *Pure and Applied Geophysics*, 157, 1663–1681.

Papazachos, B. and Papazachou, K. 2003. The earthquakes of Greece. Ziti Publications, Thessaloniki, Greece, 286 pp.

Papazachos, C. B., Karakaisis , G. F., Scordilis, E. M. & Papazachos, B. C., 2005. Global observational properties of the critical earthquake model. *Bulletin of the Seismological Society of America*, 95(10), 1841 – 1855.

Rundle, J.B., Klein, W., Turcotte, D.L. and Malamud, B.D., 2000. Precursory Seismic Activation and Critical-point Phenomena. *Pure and Applied Geophysics*, 157, 2165–2182. https://doi.org/10.1007/PL00001079

Scholz, C.H. and Aviles, C.A. 2013. The Fractal Geometry of Faults and Faulting. In: Earthquake Source Mechanics AGU Geophysical Monograph Series, Das, S., Boatwright, J., Scholz, C.H., (Eds.), AGU 100: Washington, DC, USA, 37, 147–155.

Scordilis, E.M., Papazachos, C.B., Karakaisis, G.F. and Karakostas, V.G., 2004. Accelerating seismic crustal deformation before strong mainshocks in Adriatic and its importance for earthquake prediction. *Journal of Seismology*, 8, 57 – 70.

Sornette, A. and Sornette, D., 1990. Earthquake rupture as a critical point: consequences for telluric precursors. *Tectonophysics*, 179, 327 - 334.

Tsallis, C., 2009. Introduction to Nonextensive Statistical Mechanics - Approaching a Complex World. Springer- Verlag, New York, 382 pp., doi: 10.1007/978-0-387-85359-8

Vallianatos F., Michas G., Papadakis G. 2016. A Description of Seismicity Based on Non-extensive Statistical Physics: A Review. In: D'Amico S. (eds) Earthquakes and Their Impact on Society. Springer Natural Hazards. Springer, Cham. https://doi.org/10.1007/978-3-319-21753-6_1

Vallianatos, F. and Chatzopoulos, G., 2018. A Complexity View into the Physics of the Accelerating Seismic Release Hypothesis: Theoretical Principles. *Entropy*, 20(10):754, doi.org/10.3390/e20100754

Wiemer, S., 2001. A software package to analyze seismicity: ZMAP. *Seismological Research Letters*, 72(3), pp.373-382 https://doi.org/10.1785/gssrl.72.3.373

Wyss, M., Wiemer, S. and Zuniga, R., 2001. ZMAP A tool for analyses of seismicity patterns, Typical Applications and Uses: A Cookbook.